

Dynamic Practical Byzantine Fault Tolerance and Its Blockchain System: A Large-Scale Markov Modeling

Yan-Xia Chang¹, Quan-Lin Li¹, Qing Wang²*, Xing-Shuo Song³

¹School of Economics and Management

Beijing University of Technology, Beijing 100124, China

²Monash Business School, Monash University

900 Dandenong Road Caulfield East, 3145, VIC, Australia

³School of Economics and Management

Yanshan University, Qinhuangdao 066004, China

October 26, 2022

Abstract

In a practical Byzantine fault tolerance (PBFT) blockchain network, the voting nodes may always leave the network while some new nodes can also enter the network, thus the number of voting nodes is constantly changing. Such a new PBFT with dynamic nodes is called a dynamic PBFT. Clearly, the dynamic PBFT can more strongly support the decentralization and distributed structure of blockchain. However, analyzing dynamic PBFT blockchain systems will become more interesting and challenging.

In this paper, we propose a large-scale Markov modeling technique to analyze the dynamic PBFT voting processes and its dynamic PBFT blockchain system. To this end, we set up a large-scale Markov process (and further a multi-dimensional Quasi-Birth-and-Death (QBD) process) and provide performance analysis for both the dynamic PBFT voting processes and the dynamic PBFT blockchain system. In particular, we obtain an effective computational method for the throughput of the complicated dynamic PBFT blockchain system. Finally, we use numerical examples

*Corresponding author: Q. Wang (qing.wang1@monash.edu)

This work has been submitted to the IEEE for possible publication. Copyright may be transferred without notice, after which this version may no longer be accessible.

to check the validity of our theoretical results and indicate how some key system parameters influence the performance measures of the dynamic PBFT voting processes and of the dynamic PBFT blockchain system. Therefore, by using the theory of multi-dimensional QBD processes and the RG-factorization technique, we hope that the methodology and results developed in this paper shed light on the study of dynamic PBFT blockchain systems such that a series of promising research can be developed potentially.

Keywords: Blockchain; Practical Byzantine fault tolerance (PBFT); Dynamic PBFT; QBD process; RG-factorization; Queueing system; Performance evaluation.

1 Introduction

Blockchain technologies originated in Bitcoin by Nakamoto [46] in 2008. Since then, Blockchain has attracted tremendous attention from both research communities and industrial applications. Furthermore, many real applications of blockchain benefit from a number of salient and excellent features, for example, decentralization, distributed structure, availability, persistency, consistency, anonymity, immutability, auditability, and accountability. So far, blockchain has been envisioned as a powerful backbone/framework for decentralized data processing and data-driven autonomous organization in a peer-to-peer and open-access network. Readers may refer to books by Narayanan et al. [48], Bashir [5], Raj [60], Maleh et al. [42], Rehan and Rehmani [61] and Schar and Berentsen [65]; and survey papers by Wang et al. [74], Gorkhali et al. [25], Belchior et al. [6] and Huang et al. [28]; and further survey papers with several real areas by Fauziah et al. [19] for smart contracts, Dai et al. [15] for Internet of Things (IoT), Sharma et al. [67] for cloud computing, Gorbunova et al. [24] for industrial applications, and Ekramifard et al. [16] for artificial intelligence (AI).

Consensus mechanisms always play a pivotal role in developing blockchain technologies. Up to now, there have been more than 50 different consensus mechanisms in the study of blockchain technologies. We refer readers to recent survey papers by, for example, Cachin and Vukolić [10], Bano et al. [4], Natoli et al. [49], Chaudhry and Yousaf [14], Nguyen and Kim [51], Ongaro and Ousterhout [56], Salimitari and Chatterjee [64], Wang et al. [74], Pahlajani et al. [58], Nguyen et al. [52], Carrara et al. [11], Wan et al. [73], Xiao et al. [75], Ferdous et al. [20], Nijse and Litchfield [53], Leonardos et al. [35], Yao et

al. [77], Lashkari and Musilek [34], Fu et al. [21], Khamar and Patel [30], Oyinloye et al. [57], Bains [3] and Xiong et al. [76].

For a reliable distributed computer system, the consensus result of its components reaching an agreement on a certain state is the most fundamental and important issue. To achieve consistency, a reliable distributed computer system must be able to cope with the failure of one or more of its components, in case a failed component can send conflicting information to different parts of the computer system. To solve the type of failure and conflicting problems, an important concept: *Byzantine generals problem*, is developed, e.g., see Lamport et al. [33], Lamport [32], Schlichting and Schneider [66], Reischuk [62] and Martin and Alvisi [44] for more details. Based on the Byzantine generals problem, Pease et al. [59] and Lamport et al. [33] proposed the Byzantine fault tolerant consensus mechanism (BFT), and further research includes Thai et al. [71], Li et al. [40], Zhan et al. [78] and so on.

Unfortunately, the original BFT has the problems of low algorithm efficiency, small node capacity and weak scalability. To solve these problems, Castro and Liskov [12] improve the BFT and proposed the PBFT (Practical Byzantine Fault Tolerance consensus mechanism), which makes the BFT feasible in many practical applications. Thereafter, some researchers further developed the BFT to improve the performance of the BFT or PBFT effectively. Important examples include Castro and Liskov [13], Veronese et al. [72], Abraham et al. [1], Hao et al. [27], Gueta et al. [26], Malkhi et al. [43], Sakho et al. [63], Nischwitz et al. [54], Oliveira et al. [55] and so on. Up to now, the BFT and PBFT have become the most basic ones in all the blockchain consensus mechanisms, and both play a crucial role in extending, generalizing, and finding new effective blockchain consensus mechanisms. On the research line, noteworthy examples include Kiayias and Russell [31], Bravo et al. [7], Meshcheryakov et al. [45], Alqahtani and Demirbas [2], Ma et al. [41], Garcia et al. [22], Navaroj et al. [47] and so forth.

Different from those works in the literature, a key purpose of this paper is to further propose and develop a new PBFT consensus mechanism in blockchain technologies, called a dynamic PBFT consensus, in which the votable nodes may always leave the PBFT network while some new nodes can also enter the PBFT network. In this case, the number of votable nodes is constantly changing, thus analysis of the dynamic PBFT is more challenging due to at least three reasons as follows:

- (a) Note that the votable nodes may always leave the PBFT network randomly, the

total number of votable nodes may become so small that the votable nodes cannot represent the legitimacy of final vote results in the PBFT network. Thus it highlights the need to establish a lower bound on the total number of votable nodes to ensure that the legally voting process of the PBFT network can be executed.

(b) Some new nodes can randomly enter the PBFT network, which further underpins the decentralization and distributed structure of blockchain in a huge P2P network range. Therefore, it is obviously inappropriate to design a fixed number of voting nodes in the PBFT network. In addition, too many nodes entering the network will exceed the capacity of the network, so setting up an upper bound to realize the voting processes smoothly is a requisite in the PBFT network.

(c) The major node and slave nodes deal with each transaction package through three stages of parallel voting processes: Prepare, commit, and reply. Thus, it is always challenging and complex to analyze such three-phase parallel PBFT voting processes. See Ma et al. [41] for more details.

Based on the above analysis, it is important to study the dynamic PBFT voting processes, and to provide performance evaluation of the dynamic PBFT blockchain system. To this end, we propose a large-scale Markov modeling technique to analyze the dynamic PBFT voting processes and its dynamic PBFT blockchain system. We first set up a large-scale Markov process whose elements are given a detailed discussion related to the dynamic PBFT. Then we provide key performance measures of the dynamic PBFT voting processes. Furthermore, we construct an approximate queueing model to discuss the dynamic PBFT blockchain system and provide its performance analysis. It is worthwhile to note that we provide a novel method to compute the throughput of the dynamic PBFT blockchain system. Finally, we use numerical examples to verify the validity of our theoretical results.

Note that Hao et al. [27], Ma et al. [41], and Nischwitz et al. [54] are three closely related works to our paper. Hao et al. [27] presented the dynamic PBFT network in which some nodes may enter or leave the PBFT network by means of the consensus protocols: Using the JOIN and EXIT protocols leads to some dynamic nodes. It is worthwhile to note that Hao et al. [27] is different from our work given in this paper, we describe and analyze the dynamic (entering and leaving) behavior of some nodes in the PBFT network through using the Markov process theory or random dynamical system. Ma et al. [41] considered a special case of this paper (i.e., the voters are fixed) by means of a two-dimensional Markov process. Nischwitz et al. [54] introduced a probabilistic model for

evaluating BFT protocols in the presence of dynamic link and crash failures. Their analysis is different from our large-scale Markov modeling technique developed in this paper, we observe the dynamic behavior of some nodes and provide performance evaluation of the dynamic PBFT blockchain system by means of the Markov process theory. By comparing the two studies, it is easy to see that our large-scale Markov modeling technique is superior to their probabilistic analysis method not only from the dynamic systems but also from the performance evaluation.

The Markov processes and queueing theory play a key role in the study of blockchain systems. Readers can refer to survey papers by, for example, Smetanin et al. [68], Fan et al. [18], and Huang et al. [28]. Up to now, some papers have applied the Markov processes (or Markov chains) to study the blockchain systems. For example, a transition-construction Markov chain by Eyal and Sirer [17], Markov queueing models by Li et al. [38, 39], a two-dimensional Markov process by Göbel et al. [23], a new computational method further developed by Javier and Fralix [29], a pyramid Markov processes by Li et al. [37], and a Markov process of DAG-based blockchain systems by Song et al. [69].

Based on the above analysis, the main contributions of this paper are summarized as follows:

1. This paper proposes a novel dynamic PBFT, where the votable nodes may always leave the network while new nodes may also enter the network, thus the number of votable nodes is constantly changing. Compared with the ordinary PBFT, the analysis of the dynamic PBFT is more interesting and challenging. To do this, we propose a large-scale Markov modeling technique to analyze the dynamic PBFT voting processes and dynamic PBFT blockchain system.
2. For the dynamic PBFT voting processes, we set up a large-scale QBD process and obtain its stationary probability vector, which is used to numerically compute performance measures of the dynamic PBFT voting processes. Accordingly, we establish an approximate queueing model to discuss the dynamic PBFT blockchain system and provide a new method to analyze performance of the dynamic PBFT blockchain system.
3. We use numerical examples to check the validity of our theoretical results and indicate how some key system parameters influence performance measures of the dynamic PBFT voting processes and the dynamic PBFT blockchain system.

The rest of this paper is organized as follows. Section 2 describes stochastic models for the dynamic PBFT voting processes and the dynamic PBFT blockchain system. Section 3 sets up a large-scale QBD process to express the dynamic PBFT voting processes. Section 4 obtains the stationary probability vector of the large-scale QBD process and provides performance measures of the dynamic PBFT voting processes. Section 5 establishes an approximate queueing model to discuss the dynamic PBFT blockchain system and provides a new method to compute the throughput of the dynamic PBFT blockchain system. Section 6 provides two effective algorithms for computing the throughput of the dynamic PBFT blockchain system. Section 7 uses some numerical examples to verify the validity of our theoretical results and demonstrates how the performance measures are influenced by some key system parameters. Some concluding remarks are given in Section 8.

2 Model Description of the Dynamic PBFT

In this section, we provide a detailed model description for the dynamic PBFT with entering and leaving nodes. Furthermore, we give mathematical notation, random factors, and necessary parameters used in our subsequent study.

In a dynamic PBFT, some nodes can always enter and leave the PBFT network. In this situation, the number of votable nodes may be unfixed. Therefore, how to describe and study such a dynamic PBFT becomes more interesting and challenging.

Now, we describe the dynamic PBFT with entering and leaving nodes as follows:

(1) Nodes enter the PBFT network: We assume that some external nodes entering the PBFT network follow a Poisson process with arrival rate $\mu > 0$. Obviously, the newly entering nodes increase the number of votable nodes, so that the number of over two-thirds valid votes will also increase.

(2) Nodes leave the PBFT network: We assume that the time of each valid voting node spent in the PBFT network is exponential with mean $1/\theta > 0$. Such a random time indicates that all nodes have an impatient behavior that results from multiple reasons. For example, some nodes suddenly go offline, some nodes change interest in participating in such voting, some nodes are forcibly removed from the PBFT network, and so forth.

(3) A lower threshold is required for the minimal number of valid voting nodes: Because the number of votable nodes changes randomly, we must require a lower threshold for the minimal number of votable nodes. Such a lower threshold is used to

guarantee the security of the dynamic PBFT voting process, that is, the dynamic PBFT voting process must have a sufficient number of nodes to vote and reach a consensus. We assume that the lower threshold is \mathcal{M} . If over \mathcal{M} nodes vote and reach a consensus, then the dynamic PBFT voting process is legal so that the voting results can be accepted.

(4) An upper threshold for the maximal number of valid voting nodes:

For the convenience of analysis, we set an upper threshold for the maximum number of valid voting nodes to avoid the infinite expansion of PBFT network size when the external nodes constantly enter. Meanwhile, our purpose is to avoid some complicated theoretical discussion for a large-scale Markov model of the dynamic PBFT voting process, for example, stability analysis, and computation of the stationary probability vector. We assume that the upper threshold is \mathcal{N} . When the number of valid voting nodes reaches the upper threshold \mathcal{N} , any new arriving external node can no longer enter the PBFT network.

(5) The probability that the transaction package is approved or refused by the valid voting nodes: To simplify the analysis, we assume that all valid voting nodes are identical when a transaction package is submitted to each node for voting. In this paper, we do not distinguish the properties of valid voting nodes, such as Byzantine or non-Byzantine. Furthermore, we assume that the voting time of each node is exponential with mean $1/\gamma > 0$; and the probability that a transaction package is approved by each node is p , while the probability that a transaction package is refused by each node is $q = 1 - p$.

(6) The judgment of the voting result: We denote by $N(t)$, $M(t)$, and $K(t)$ the number of valid voting nodes, the number of nodes that approve the transaction package, and the number of nodes that refuse the transaction package at time t , respectively. $N(t) - M(t) - K(t)$ is the number of nodes that have not completed their voting processes yet. We assume that **(a)** a transaction package becomes a block if $M(t) > (2/3) \cdot N(t)$ and $M(t) \geq \mathcal{M}$; and **(b)** the transaction package becomes an orphan block if $M(t) \leq (2/3) \cdot N(t)$ and $M(t) \geq \mathcal{M}$, and it is returned to the transaction pool (i.e., rollback).

(7) The times of block-pegging and rolling-back: The block-pegging time is a time interval from the completion time of the voting and consensus to the epoch that the block is pegged on the blockchain. Also, the rolling-back time is also a time interval from the completion time of voting and consensus to the epoch that the orphan block is returned to the transaction pool.

Note that the times of block-pegging and rolling-back are mainly determined by the network latency of the dynamic PBFT system, both of them are identical. In this case, we assume that the block-pegging time and rolling-back time are exponential with the same mean $1/\beta$.

(8) Transaction arrivals at the transaction pool: To study the dynamic PBFT blockchain system (see Section 5), we assume that arrivals of transactions follow a Poisson process with arrival rate $\lambda > 0$, and the capacity of the transaction pool is infinite.

(9) Independence: We assume that all random variables defined above are independent of each other.

Remark 1 *When $\mathcal{M} \leq N(t) \leq \mathcal{N}$, for each positive integer $N(t)$, there exist a positive integer k such that $N(t) = 3k, 3k + 1, 3k + 2$. In fact, we can find that checking (a) and (b) in Assumption (6) is not easy for some integers, and it is necessary and useful for considering the following cases: (1) If $N(t) = 3k$ or $N(t) = 3k + 1$, $M(t) \geq 2k + 1$; and (2) If $N(t) = 3k + 2$, $M(t) \geq 2k + 2$. Based on this, we write*

$$m_l = \begin{cases} 2k + 1, & N(t) = 3k \text{ or } N(t) = 3k + 1, \\ 2k + 2, & N(t) = 3k + 2. \end{cases} \quad (1)$$

$$k_l = \begin{cases} k, & N(t) = 3k, \\ k + 1, & N(t) = 3k + 1 \text{ or } N(t) = 3k + 2. \end{cases} \quad (2)$$

If $M(t) \geq m_l$, then the transaction package becomes a block; and if $K(t) \geq k_l$, then the transaction package becomes an orphan block, which is returned to the transaction pool.

Remark 2 *In our dynamic PBFT voting process, we describe the voting behavior of Byzantine nodes from a probabilistic perspective, which is reasonable by means of a statistical approach.*

3 A QBD Process for Dynamic PBFT Voting Process

In this section, we set up a three-dimensional continuous-time Markov model to analyze the dynamic PBFT voting process, and further formulate it as a QBD process with finite states.

Note that $N(t)$, $M(t)$, and $K(t)$ denote the number of valid voting nodes, the number of valid voting nodes that approve the transaction package, and the number of valid voting

nodes that refuse the transaction package at time t , respectively; and $N(t) - M(t) - K(t)$ is the number of valid voting nodes that have not completed their voting process yet.

For convenience of analysis, we take that $\mathcal{M} = 3L$ and $\mathcal{N} = 3N + 2$, where L and N are two fixed constants, and $N \gg L$.

It is clear that $\{(N(t), M(t), K(t)) : t \geq 0\}$ is a three-dimensional continuous-time Markov process, whose state space is given by

$$\Theta = \{(l, 0, 0) : 0 \leq l \leq 3L - 1\} \cup \left\{ \bigcup_{k=L}^N \text{Level } k \right\}, \quad (3)$$

where

$$\text{Level } k = \text{Sublevel}_{k,0} \cup \text{Sublevel}_{k,1} \cup \text{Sublevel}_{k,2},$$

$$\begin{aligned} \text{Sublevel}_{k,0} = & \{(3k, 0, 0), (3k, 0, 1), \dots, (3k, 0, 3k - 2), (3k, 0, 3k - 1), (3k, 0, 3k); \\ & (3k, 1, 0), (3k, 1, 1), \dots, (3k, 1, 3k - 2), (3k, 1, 3k - 1); \\ & (3k, 2, 0), (3k, 2, 1), \dots, (3k, 2, 3k - 2); \dots; \\ & (3k, 3k, 0)\}, \end{aligned}$$

$$\begin{aligned} \text{Sublevel}_{k,1} = & \{(3k + 1, 0, 0), (3k + 1, 0, 1), \dots, (3k + 1, 0, 3k), (3k + 1, 0, 3k + 1); \\ & (3k + 1, 1, 0), (3k + 1, 1, 1), \dots, (3k + 1, 1, 3k - 1), (3k + 1, 1, 3k); \\ & (3k + 1, 2, 0), (3k + 1, 2, 1), \dots, (3k + 1, 2, 3k - 1); \dots; \\ & (3k + 1, 3k + 1, 0)\}, \end{aligned}$$

$$\begin{aligned} \text{Sublevel}_{k,2} = & \{(3k + 2, 0, 0), (3k + 2, 0, 1), \dots, (3k + 2, 0, 3k + 1), (3k + 2, 0, 3k + 2); \\ & (3k + 2, 1, 0), (3k + 2, 1, 1), \dots, (3k + 2, 1, 3k), (3k + 2, 1, 3k + 1); \\ & (3k + 2, 2, 0), (3k + 2, 2, 1), \dots, (3k + 2, 2, 3k); \dots; \\ & (3k + 2, 3k + 2, 0)\}. \end{aligned}$$

The state transition relations between any two levels are depicted in Figure 1, and the state transitions in each sub-level are depicted in Figures 2 to 4. Note that the complicated structure of the state transition is due to the fact that some nodes can enter and leave the PBFT network.

From Figure 1 to 4, it is easy to see that

$$N(t) \in \{0, 1, 2, \dots, 3L - 1; 3L, 3L + 1, 3L + 2; \dots; 3N, 3N + 1, 3N + 2\},$$

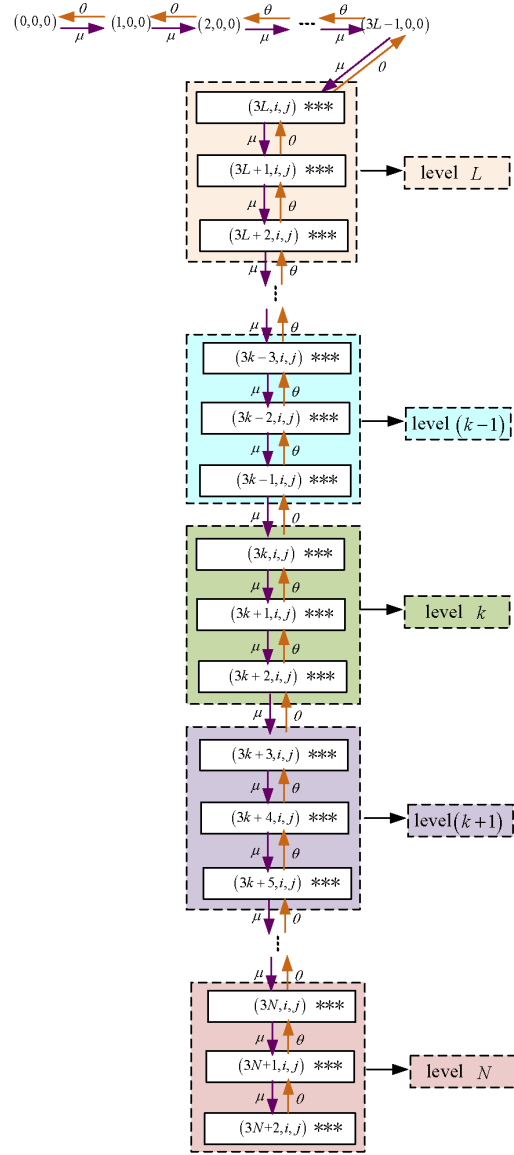


Figure 1: The state transition relations between any two levels.

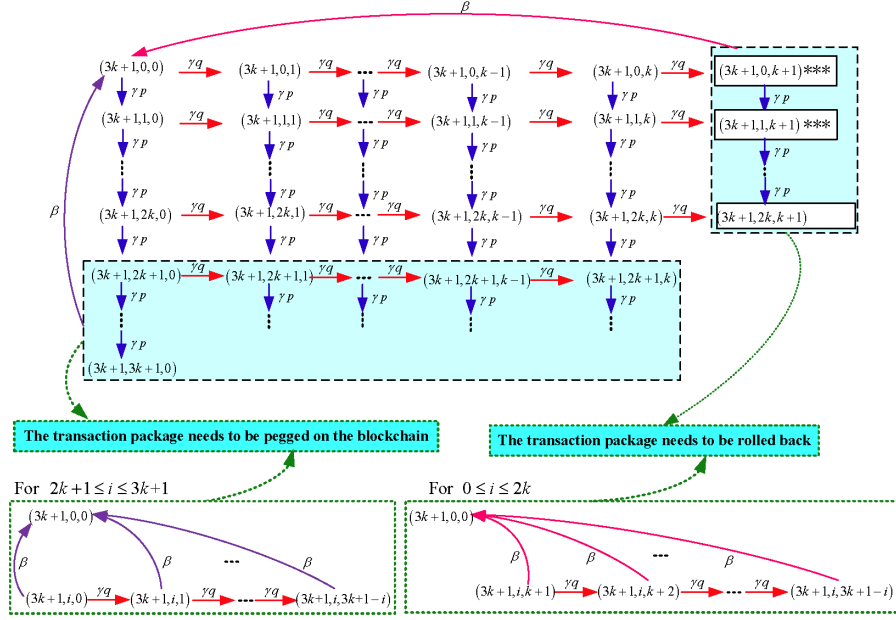


Figure 3: The state transition relations in Sublevel_{k,1}.

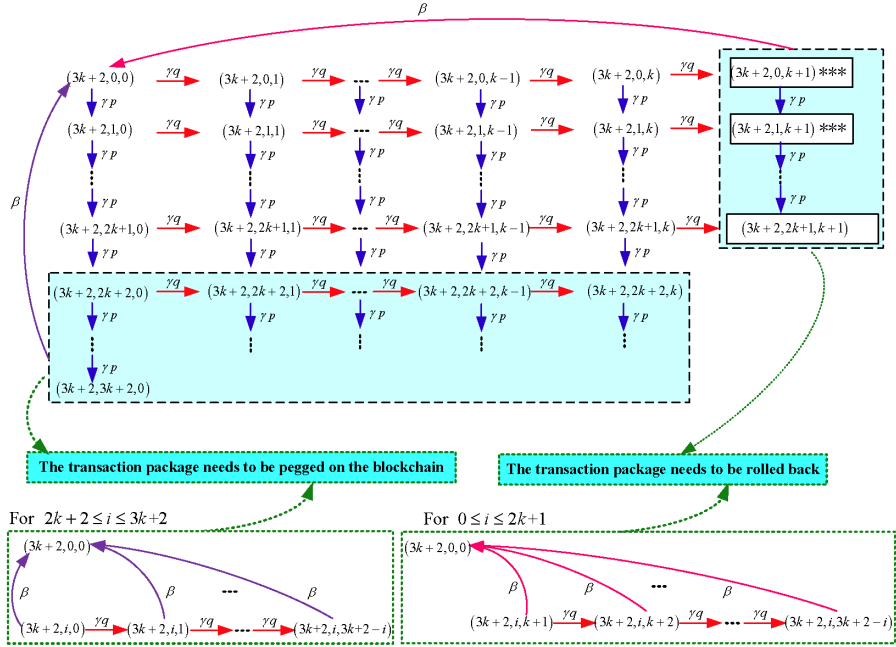


Figure 4: The state transition relations in Sublevel_{k,2}.

for $3L \leq l \leq 3N + 1$,

$$Q_0^{(l)} = \begin{pmatrix} A_{0,0} & & & \\ & A_{1,1} & & \\ & & \ddots & \\ & & & A_{l,l} & 0 \end{pmatrix},$$

$$A_{i,i} = \begin{pmatrix} \mu & & & \\ & \mu & & \\ & & \ddots & \\ & & & \mu & 0 \end{pmatrix}_{(l+1-i) \times (l+2-i)}, \quad 0 \leq i \leq l;$$

for $3L + 1 \leq l \leq 3N + 2$,

$$Q_2^{(l)} = \begin{pmatrix} B_{0,0} & & & \\ & B_{1,1} & & \\ & & \ddots & \\ & & & B_{l-1,l-1} \\ & & & & 0 \end{pmatrix},$$

$$B_{j,j} = \begin{pmatrix} \theta & & & \\ & \theta & & \\ & & \ddots & \\ & & & \theta \\ & & & & 0 \end{pmatrix}_{(l+1-j) \times (l-j)}, \quad 0 \leq j \leq l-1;$$

$$Q_2^{(3L)} = \begin{pmatrix} \tilde{Q}_{0,0} \\ 0 \\ \vdots \\ 0 \end{pmatrix},$$

$$\tilde{Q}_{0,0} = \begin{pmatrix} 0 & \cdots & 0 & \theta \\ 0 \\ \vdots \\ 0 \end{pmatrix}_{(3L+1) \times (3L)};$$

for $l = 3L$,

$$G_{0,0} = \begin{pmatrix} -(\gamma + \mu + \beta) & \gamma q & & & \\ & \ddots & \ddots & & \\ & & -(\gamma + \mu + \beta) & \gamma q & \\ & & & -(\mu + \beta) & \\ & & & & \end{pmatrix}_{(2L+1) \times (2L+1)},$$

$$D_{0,0} = \begin{pmatrix} -(\gamma + \mu + \theta) & \gamma q & & & \\ & -(\gamma + \mu) & \gamma q & & \\ & & \ddots & \ddots & \\ & & & -(\gamma + \mu) & \gamma q \\ & & & & \end{pmatrix}_{L \times (3L+1)},$$

for $l = 3N + 2$,

$$G_{0,0} = \begin{pmatrix} -(\gamma + \theta + \beta) & \gamma q & & & \\ & \ddots & \ddots & & \\ & & -(\gamma + \theta + \beta) & \gamma q & \\ & & & -\beta & \\ & & & & \end{pmatrix}_{(2N+2) \times (2N+2)};$$

$$D_{0,0} = \begin{pmatrix} -(\gamma + \theta) & \gamma q & & & \\ & -(\gamma + \theta) & \gamma q & & \\ & & \ddots & \ddots & \\ & & & -(\gamma + \theta) & \gamma q \\ & & & & \end{pmatrix}_{(N+1) \times (3N+3)},$$

for $r = 1, 2, \dots, m_l - 2$,

$$C_{r,0} = \begin{pmatrix} 0 \\ H_{r,0} \end{pmatrix}_{(l+1-r) \times (l+1)}, \quad H_{r,0} = \begin{pmatrix} \beta \\ \beta \\ \vdots \\ \beta \end{pmatrix}_{(l+1-k_l-r) \times (l+1)},$$

$$C_{r,r} = \begin{pmatrix} I_{r,r} \\ J_{r,r} \end{pmatrix}, \quad J_{r,r} = \begin{pmatrix} 0 & K_{r,r} \end{pmatrix},$$

$$I_{r,r} = \begin{pmatrix} -(\gamma + \theta + \mu) & \gamma q & & & \\ & -(\gamma + \theta + \mu) & \gamma q & & \\ & & \ddots & \ddots & \\ & & & -(\gamma + \theta + \mu) & \gamma q \\ & & & & \end{pmatrix}_{k_l \times (l+1-r)},$$

$$K_{r,r} = \begin{pmatrix} -(\gamma + \mu + \theta + \beta) & \gamma q & & \\ & \ddots & \ddots & \\ & & -(\gamma + \mu + \theta + \beta) & \gamma q \\ & & & -(\mu + \beta) \end{pmatrix}_{(l+1-k_l-r) \times (l+1-k_l-r)},$$

for $l = 3L$,

$$I_{r,r} = \begin{pmatrix} -(\gamma + \mu) & \gamma q & & \\ & -(\gamma + \mu) & \gamma q & \\ & & \ddots & \ddots \\ & & & -(\gamma + \mu) & \gamma q \end{pmatrix}_{L \times (3L+1-r)},$$

$$K_{r,r} = \begin{pmatrix} -(\gamma + \mu + \beta) & \gamma q & & \\ & \ddots & \ddots & \\ & & -(\gamma + \mu + \beta) & \gamma q \\ & & & -(\mu + \beta) \end{pmatrix}_{(2L+1-r) \times (2L+1-r)},$$

for $l = 3N + 2$,

$$I_{r,r} = \begin{pmatrix} -(\gamma + \theta) & \gamma q & & \\ & -(\gamma + \theta) & \gamma q & \\ & & \ddots & \ddots \\ & & & -(\gamma + \theta) & \gamma q \end{pmatrix}_{(N+1) \times (3N+3-r)},$$

$$K_{r,r} = \begin{pmatrix} -(\gamma + \theta + \beta) & \gamma q & & \\ & \ddots & \ddots & \\ & & -(\gamma + \theta + \beta) & \gamma q \\ & & & -\beta \end{pmatrix}_{(2N+2-r) \times (2N+2-r)};$$

for $r = m_l - 1$,

$$C_{r,0} = \begin{pmatrix} \beta \end{pmatrix}_{(l+1-r) \times (l+1)},$$

$$C_{r,r} = \begin{pmatrix} -(\gamma + \mu + \theta) & \gamma q & & \\ & \ddots & \ddots & \\ & & -(\gamma + \mu + \theta) & \gamma q \\ & & & -(\mu + \beta) \end{pmatrix}_{(l+1-r) \times (l+1-r)},$$

for $l = 3L$,

$$C_{r,r} = \begin{pmatrix} -(\gamma + \mu) & \gamma q & & & \\ & -(\gamma + \mu) & \gamma q & & \\ & & \ddots & \ddots & \\ & & & -(\gamma + \mu) & \gamma q \\ & & & & -(\mu + \beta) \end{pmatrix}_{(3L+1-r) \times (3L+1-r)},$$

for $l = 3N + 2$,

$$C_{r,r} = \begin{pmatrix} -(\gamma + \theta) & \gamma q & & & \\ & \ddots & \ddots & & \\ & & -(\gamma + \theta) & \gamma q & \\ & & & -(\gamma + \theta) & \gamma q \\ & & & & -\beta \end{pmatrix}_{(l+1-r) \times (l+1-r)} ;$$

for $m_l \leq r \leq l - 1$,

$$C_{r,0} = \begin{pmatrix} \beta \\ \vdots \\ \beta \end{pmatrix}_{(l+1-r) \times (l+1)},$$

$$C_{r,r} = \begin{pmatrix} -(\gamma + \mu + \theta + \beta) & \gamma q & & & \\ & \ddots & \ddots & & \\ & & -(\gamma + \mu + \theta + \beta) & \gamma q & \\ & & & -(\mu + \beta) & \\ & & & & -(\mu + \beta) \end{pmatrix}_{(l+1-r) \times (l+1-r)},$$

for $l = 3L$,

$$C_{r,r} = \begin{pmatrix} -(\gamma + \mu + \beta) & \gamma q & & & \\ & -(\gamma + \mu + \beta) & \gamma q & & \\ & & \ddots & \ddots & \\ & & & -(\gamma + \mu + \beta) & \gamma q \\ & & & & -(\mu + \beta) \end{pmatrix}_{(l+1-r) \times (l+1-r)},$$

Note that the stationary probability vector $\boldsymbol{\pi}$ can be obtained by means of solving the system of linear equations $\boldsymbol{\pi}Q = \mathbf{0}$ and $\boldsymbol{\pi}\mathbf{e} = 1$, where \mathbf{e} is a column vector of the ones with a suitable size.

Now, we use the UL-type RG-factorization to compute the stationary probability vector $\boldsymbol{\pi}$ as follows.

We write

$$U_{3N+2} = Q_1^{(3N+2)}, \quad (6)$$

$$U_k = Q_1^{(k)} + Q_0^{(k)} (-U_{k+1}^{-1}) Q_2^{(k+1)}, \quad 3L \leq k \leq 3N+1, \quad (7)$$

$$U_0 = Q_1^{(0)} + Q_0^{(0)} (-U_{3L}^{-1}) Q_2^{(3L)}. \quad (8)$$

Based on the U-measure $\{U_k\}$, we can respectively define the UL-type R- and G-measures as

$$R_0 = Q_0^{(0)} (-U_{3L}^{-1}), \quad (9)$$

$$R_k = Q_0^{(k)} (-U_{k+1}^{-1}), \quad 3L \leq k \leq 3N+1, \quad (10)$$

and

$$G_k = (-U_k^{-1}) Q_2^{(k)}, \quad 3L \leq k \leq 3N+2. \quad (11)$$

Note that the matrix sequence $\{R_0, R_{3L}, R_{3L+1}, \dots, R_{3N}\}$ is the unique nonnegative solution to the system of matrix equations

$$\begin{cases} Q_0^{(0)} + R_0 Q_1^{(3L)} + R_0 R_{3L} Q_2^{(3L+1)} = 0, \\ Q_0^{(k)} + R_k Q_1^{(k+1)} + R_k R_{k+1} Q_2^{(k+2)} = 0, \quad 3L \leq k \leq 3N, \end{cases}$$

with the boundary condition

$$R_{3N+1} = Q_0^{(3N+1)} (-U_{3N+2}^{-1}).$$

Hence we obtain

$$\begin{cases} R_0 = -Q_0^{(0)} \left[Q_1^{(3L)} + R_{3L} Q_2^{(3L+1)} \right]^{-1}, \\ R_k = -Q_0^{(k)} \left[Q_1^{(k+1)} + R_{k+1} Q_2^{(k+2)} \right]^{-1}, \quad 3L \leq k \leq 3N. \end{cases}$$

Similarly, the matrix sequence $\{G_k, 3L \leq k \leq 3N+1\}$ is the unique nonnegative solution to the system of matrix equations

$$Q_0^{(k)} G_{k+1} G_k + Q_1^{(k)} G_k + Q_2^{(k)} = 0, \quad 3L \leq k \leq 3N+1,$$

determined by

$$\pi_0 \mathbf{e} + \sum_{k=3L}^{3N+2} \pi_k \mathbf{e} = 1.$$

4.2 Performance Analysis

Using the stationary probability vector π given in Theorem 1, we can provide some performance measures of the dynamic PBFT voting process as follows:

(a) **The stationary probability that the transaction package becomes a block is given by**

$$\zeta_1 = \sum_{l=3L}^{3N+2} \sum_{m \geq m_l}^l \sum_{k=0}^{l-m} \pi_{l,m,k}.$$

(b) **The stationary probability that the transaction package becomes an orphan block is given by**

$$\zeta_2 = \sum_{l=3L}^{3N+2} \sum_{m=0}^{m_l-1} \sum_{k \geq k_l}^{l-m} \pi_{l,m,k}.$$

(c) (i) **The stationary probability that the dynamic PBFT system completes the voting process is given by**

$$\mathbf{A} = \sum_{l=3L}^{3N+2} \sum_{m \geq m_l}^l \sum_{k=0}^{l-m} \pi_{l,m,k} + \sum_{l=3L}^{3N+2} \sum_{m=0}^{m_l-1} \sum_{k \geq k_l}^{l-m} \pi_{l,m,k} = \zeta_1 + \zeta_2.$$

(ii) **The stationary probability that the dynamic PBFT system cannot perform the voting process is given by**

$$\mathbf{B} = \sum_{i=0}^{3L-1} \pi_{i,0,0} = \pi_0 \mathbf{e}.$$

(iii) **The stationary probability that the dynamic PBFT system perform the voting process but it cannot complete the voting process is given by**

$$\mathbf{C} = 1 - \mathbf{A} - \mathbf{B}.$$

(d) **The stationary rate that the blocks are pegged on the blockchain is given by**

$$r_1 = \beta \left(\sum_{l=3L}^{3N+2} \sum_{m \geq m_l}^l \sum_{k=0}^{l-m} \pi_{l,m,k} \right) = \beta \zeta_1. \quad (13)$$

(e) **The stationary rate the the orphan blocks are rolled back is given by**

$$r_2 = \beta \left(\sum_{l=3L}^{3N+2} \sum_{m=0}^{m_l-1} \sum_{k \geq k_l}^{l-m} \pi_{l,m,k} \right) = \beta \zeta_2. \quad (14)$$

5 The dynamic PBFT Blockchain System

In this section, we set up an $M \oplus M^b / M^b / 1$ queue to approximately study the dynamic PBFT blockchain system. Using such an approximate queueing model, we can provide performance analysis of the dynamic PBFT blockchain system, for example, the throughput, and the growth rate of blockchain.

5.1 An approximate queueing model

Note that the dynamic PBFT blockchain system is a complicated network due to the dynamic voting processes, thus its performance analysis is always more interesting and challenging. For this reason, we design an $M \oplus M^b / M^b / 1$ queue to approximately analyze performance measures of the dynamic PBFT blockchain system. Now, the $M \oplus M^b / M^b / 1$ queue is described as follows:

(1) Transaction arrivals at the transaction pool: We assume that the external transactions arrive at the transaction pool according to a Poisson process with arrival rate $\lambda > 0$. See Assumption (8) in Section 2.

(2) The total arrival process: From (e) of Subsection 4.2, we can see that the stationary rate that all the orphan blocks are returned to the transaction pool is given by

$$r_2 = \beta \left(\sum_{l=3L}^{3N+2} \sum_{m=0}^{m_l-1} \sum_{k \geq k_l}^{l-m} \pi_{l,m,k} \right) = \beta \zeta_2$$

with a batch size b of transactions. Combining the above **(1)**, we can get that the total transaction arrivals at this system are a composite process between the two Poisson processes: One with arrival rate λ while the other with arrival rate r_2 , as well as batch size b .

(3) The service times: Note that the dynamic PBFT blockchain system randomly selects b transactions from the transaction pool with equal probability to make a new transaction package of batch size b , and then the transaction package immediately performs

through the dynamic PBFT voting process. We assume that the approval time of the transaction package in the voting process is exponential with approval rate r_1 .

From the perspective of queueing theory, the service time is exponential with approval rate r_1 and batch size b of transactions. That is, the block-pegged rate is r_1 .

(4) Independence: We assume that all random variables defined above are independent of each other.

From the above model assumptions, it is easy to see that the dynamic PBFT blockchain system is approximately described as an $M \oplus M^b/M^b/1$ queue. The $M \oplus M^b/M^b/1$ queue and its dynamic PBFT blockchain system are depicted in Figure 5.

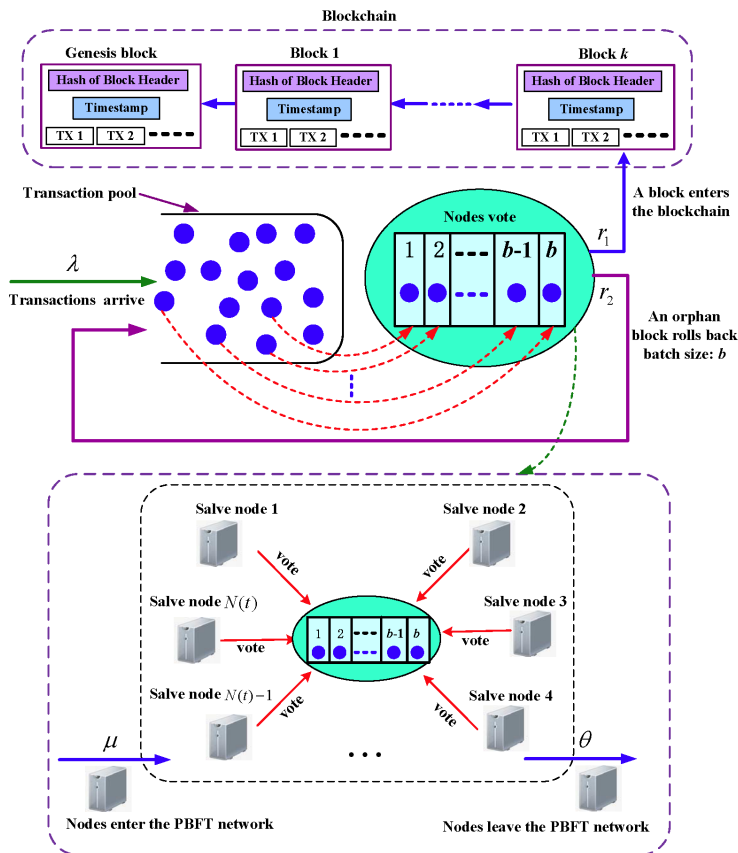


Figure 5: The $M \oplus M^b/M^b/1$ queue and its dynamic PBFT blockchain system.

Let $I(t)$ be the number of transactions in the transaction pool at time t . If $0 \leq I(t) \leq b - 1$, then a transaction package cannot be completed so that the voting process will not be set up, i.e., the dynamic PBFT system is in an idle period because there is no voting process. If $I(t) \geq b$, then the dynamic PBFT blockchain system is in a busy period.

$$T_{i,i+1} = \lambda; \quad T_{i,i+b} = r_2 \text{ if } i \geq 0; \quad T_{i,i-b} = r_1 \text{ if } i \geq b.$$

Further, the infinitesimal generator T can be rewritten as

$$\mathbf{T} = \begin{pmatrix} B_1^{(0)} & A_0 & & & \\ A_2 & A_1 & A_0 & & \\ & A_2 & A_1 & A_0 & \\ & & \ddots & \ddots & \ddots \end{pmatrix}, \quad (15)$$

where

$$B_1^{(0)} = \begin{pmatrix} -(\lambda + r_2) & \lambda & & & \\ & -(\lambda + r_2) & \lambda & & \\ & & \ddots & \ddots & \\ & & & -(\lambda + r_2) & \lambda \\ & & & & -(\lambda + r_2) \end{pmatrix},$$

$$A_0 = \begin{pmatrix} r_2 & & & & \\ & r_2 & & & \\ & & \ddots & & \\ & & & \ddots & \\ \lambda & & & & r_2 \end{pmatrix}, \quad A_2 = \begin{pmatrix} r_1 & & & & \\ & r_1 & & & \\ & & \ddots & & \\ & & & \ddots & \\ & & & & r_1 \end{pmatrix},$$

$$A_1 = \begin{pmatrix} -(\lambda + r_2 + r_1) & \lambda & & & \\ & -(\lambda + r_2 + r_1) & \lambda & & \\ & & \ddots & \ddots & \\ & & & -(\lambda + r_2 + r_1) & \lambda \\ & & & & -(\lambda + r_2 + r_1) \end{pmatrix}.$$

Obviously, the continuous-time Markov process T is a level-independent QBD process. Thus, we can apply the matrix-geometric solution to analyze the QBD process T and the dynamic PBFT blockchain system.

The following theorem provides a stability condition of the QBD process T .

Theorem 2 *The level-independent QBD T is positive recurrent if and only if*

$$\lambda + r_2 b < r_1 b.$$

Proof. For the continuous-time QBD process T , we use the mean-drift method to provide a stability condition. To use the mean-drift method, readers may refer to Chapter 1 of Neuts [50] or Chapter 3 of Li [36]. We write

$$\mathbf{A} = A_2 + A_1 + A_0 = \begin{pmatrix} -\lambda & \lambda & & & \\ & -\lambda & \lambda & & \\ & & \ddots & \ddots & \\ & & & -\lambda & \lambda \\ \lambda & & & & -\lambda \end{pmatrix}.$$

Clearly, the Markov process \mathbf{A} is irreducible, aperiodic and positive recurrent. Let φ be the stationary probability vector of Markov process \mathbf{A} , where $\varphi = (\varphi_1, \varphi_2, \dots, \varphi_b)$. Then φ is the unique solution to the system of linear equations: $\varphi \mathbf{A} = 0$ and $\varphi \mathbf{e} = 1$. It is easy to check that $\varphi_1 = \varphi_2 = \dots = \varphi_b = 1/b$.

Using the mean-drift method, it is well-known that the QBD process T is positive recurrent if and only if

$$\varphi A_0 \mathbf{e} < \varphi A_2 \mathbf{e}.$$

Note that

$$\varphi A_0 \mathbf{e} = \frac{\lambda + r_2 b}{b}, \quad \varphi A_2 \mathbf{e} = r_1,$$

this gives

$$\lambda + r_2 b < r_1 b.$$

Therefore, the QBD process T is positive recurrent if and only if

$$\lambda + r_2 b < r_1 b.$$

This completes the proof. \square

When the QBD process T is positive recurrent, we write its stationary probability vector as

$$\boldsymbol{\omega} = (\omega_0, \omega_1, \omega_2, \dots),$$

where

$$\omega_k = (\omega_{kb}, \omega_{kb+1}, \dots, \omega_{(k+1)b-1}), \quad k \geq 0.$$

Note that the stationary probability vector $\boldsymbol{\omega}$ in general has not an explicit expression, thus we need to develop some numerical solution to the vector $\boldsymbol{\omega}$. To this end, it is easy

to see from Chapter 3 of Neuts [50] that we first need to numerically compute the rate matrix R , which is the minimal nonnegative solution to the nonlinear matrix equation $R^2A_2 + RA_1 + A_0 = 0$. In addition, the rate matrix R can be numerically calculated by an iterative algorithm (see Chapter 3 of Neuts [50]) as follows:

$$R_0 = 0,$$

and

$$R_{n+1} = (R_n^2A_2 + A_0)(-A_1^{-1}), \quad n = 1, 2, 3, \dots \quad (16)$$

For the matrix sequence $\{R_n, n \geq 0\}$, it is easy to see that $R(n) \uparrow R$ as $n \rightarrow \infty$ by means of the Chapter 3 of Neuts [50], thus, for any sufficiently small positive number ε , there exists a positive integer \mathbf{n} such that

$$\|R_{\mathbf{n}+1} - R_{\mathbf{n}}\| < \varepsilon. \quad (17)$$

In this case, we take $R \approx R_{\mathbf{n}}$, which gives an approximate solution to the nonlinear matrix equation $R^2A_2 + RA_1 + A_0 = 0$.

The following theorem provides expression for the stationary probability vector $\boldsymbol{\omega}$, which directly comes from Theorem 1.2.1 of Chapter 1 in Neuts [50]. Here, we restate it without a proof.

Theorem 3 *If the QBD process T is positive recurrent, then its stationary probability vector $\boldsymbol{\omega} = (\omega_0, \omega_1, \omega_2, \dots)$ is given by*

$$\omega_k = \omega_1 R^{k-1}, \quad k \geq 1, \quad (18)$$

where ω_0 and ω_1 are the unique solution to the following system of linear equations:

$$\begin{cases} \omega_0 A_1^{(0)} + \omega_1 A_2 = 0, \\ \omega_0 A_0 + \omega_1 (A_1 + RA_2) = 0, \\ \omega_0 \mathbf{e} + \omega_1 (I - R)^{-1} \mathbf{e} = 1. \end{cases} \quad (19)$$

5.3 Performance analysis of the PBFT blockchain system

Based on the $M \oplus M^b / M^b / 1$ queue and the stationary probability vector $\boldsymbol{\omega}$, we provide some key performance measures of the PBFT blockchain system as follows:

(a) (i) **The stationary probability of no transaction package in the dynamic PBFT blockchain system** is given by

$$\eta_1 = \omega_0 \mathbf{e}. \quad (20)$$

(ii) **The stationary probability of existing transaction package in the dynamic PBFT blockchain system** is given by

$$\eta_2 = 1 - \eta_1 = 1 - \omega_0 \mathbf{e}.$$

(b) (i) **The stationary rate that a block is pegged on the blockchain in the dynamic PBFT blockchain system** is given by

$$\mathfrak{R}_1 = \beta \eta_2 \zeta_1 = \eta_2 r_1. \quad (21)$$

(ii) **The stationary rate that an orphan block is returned to the transaction pool** is given by

$$\mathfrak{R}_2 = \beta \eta_2 \zeta_2 = \eta_2 r_2.$$

Now, we provide an effective method to compute the throughput of the dynamic PBFT blockchain system.

Theorem 4 *The transaction throughput of the dynamic PBFT blockchain system is given by*

$$\text{TH} = \mathfrak{R}_1 b. \quad (22)$$

Proof. From Figure 6, it is seen that the block throughput of the dynamic PBFT blockchain system is given by

$$\begin{aligned} \text{TH}_{\text{block}} &= \text{The stationary rate that a block is pegged on the blockchain} \\ &\quad \times \text{The stationary probability that a block is pegged on the blockchain,} \end{aligned}$$

this gives

$$\text{TH}_{\text{block}} = r_1 \sum_{k=1} \omega_k e = r_1 (1 - \omega_0 \mathbf{e}) = r_1 \eta_2 = \mathfrak{R}_1.$$

Thus, the transaction throughput of the dynamic PBFT blockchain system is given by

$$\text{TH} = b \text{TH}_{\text{block}} = \mathfrak{R}_1 b.$$

This completes the proof. \square

Remark 5 *The dynamic PBFT blockchain system is a very complicated stochastic system. To analyze such a complicated blockchain system, this paper develops a two-stage decomposition technique: One for the voting process corresponding to the service times; and the other for an approximate queueing system with a feedback mechanism. We find that the two-stage decomposition technique is very effective for studying the PoS (or DPoS) blockchain systems, the Raft blockchain systems and others. In particular, we provide a simple expression for evaluating the throughput of the dynamic PBFT blockchain system.*

6 Two Algorithms

In this section, we provide two effective algorithms through using the key techniques given in Bright and Taylor [8, 9] and the RG-factorizations given in Li [36]. In particular, we can numerically compute the throughput of the dynamic PBFT blockchain system.

It is worthwhile to note that the stationary rates r_1 and r_2 obtained in Section 4 are the elements of the infinitesimal generator T given in Section 5. Therefore, before calculating the throughput TH, we need to compute the stationary rates r_1 and r_2 firstly. To do this, we use the RG-factorization and the method of matrix-geometric solutions given in Neuts [50] to get the stationary rates r_1 and r_2 . Such calculation steps are shown in Algorithm 1.

Next, we use the stationary rates r_1 and r_2 obtained by Algorithm 1 to further calculate throughput TH. Note that the calculation of throughput TH depends on ω , and the calculation of ω depends on the rate matrix R . Therefore, we first need to determine the rate matrix R , and then compute throughput TH. Note that the rate matrix R can be approximately calculated by the iterative algorithm, thus, we take a controllable accuracy $\varepsilon = 10^{-12}$, and by using the equation (17), we can get the rate matrix $R \approx R_{\mathbf{n}}$ and the suitable number of iterations \mathbf{n} once the termination condition is met. When we get the suitable rate matrix R and iterative number \mathbf{n} , we can compute the η_1 and η_2 , and further we can get the approximate throughput TH accordingly. Such calculation steps are shown in Algorithm 2.

Algorithm 1: Computing the stationary rates r_1 and r_2 .

Input: The key parameters: $\mu, \theta, \gamma, \beta, p$;

Constants related to the number of nodes L and N

Output: The stationary rates: r_1, r_2

- 1 Determine transition blocks $\{Q_1^{(0)}, Q_0^{(0)}, Q_2^{(l)}, Q_1^{(l)}, Q_0^{(l)}\}$,
 $l = 3L, 3L + 1, \dots, 3N + 2$;
 - 2 Use equations (6-10) to compute U-measure, R-measure ;
 - 3 Based on the U-measure and R-measure, using $v_0 U_0 = 0$ and $v_0 \mathbf{e} = 1$, determine the vector v_0 ;
 - 4 Compute the stationary probabilities $\pi_0, \pi_k, k = 3L, 3L + 1, \dots, 3N + 2$ through the system of linear equations (12) and $\pi_0 \mathbf{e} + \sum_{k=3L}^{3N+2} \pi_k \mathbf{e} = 1$;
 - 5 Use equations (13) and (14) to compute the stationary rates r_1 and r_2 ;
 - 6 Return the stationary rates r_1 and r_2 .
-

Algorithm 2: Computing throughput of the dynamic PBFT blockchain system.

Input: The key parameters: $\mu, \theta, \gamma, \beta, p, \lambda, b$;

A controllable accuracy ε

Output: The throughput of the dynamic PBFT blockchain system: TH

- 1 Use Algorithm 1, compute the stationary rates r_1 and r_2 ;
- 2 Based on the obtained r_1, r_2 , determine the transition blocks $\{B_1^{(0)}, A_2, A_1, A_0\}$;
- 3 Use equation (16) to compute R iteratively, and stop the iteration if

$$\|R_{\mathbf{n}+1} - R_{\mathbf{n}}\| < \varepsilon ;$$

- 4 Solve ω_0 and ω_1 through the system equations (19), and then get the ω_k through equation (18), $k = 1, 2, \dots, K$;
 - 5 Compute \mathfrak{R}_1 given by equation (21) through equation (20) ;
 - 6 Compute the throughput TH through the equation (22) ;
 - 7 Return the throughput TH.
-

7 Numerical Analysis

In this section, we use two groups of numerical examples to verify the validity of our theoretical results and to show how some key system parameters influence performance measures of the dynamic PBFT voting process and its dynamic blockchain system.

Group one: The dynamic PBFT voting process

Now, we are going to observe the impact of the key parameters $\mu, \theta, \gamma, p, \beta$ on the performance measures of the dynamic PBFT voting process.

In Figure 7(a), we take the parameters as follows: $\theta = 2, \beta = 2, \gamma = 10, p \in [0.4, 0.7]$ and $\mu = 1.85, 2, 2.5$. In Figure 7(b), we take the parameters as follows: $\mu = 2, \beta = 2, \gamma = 10, p \in [0.3, 0.75]$, and $\theta = 2, 2.5, 3$.

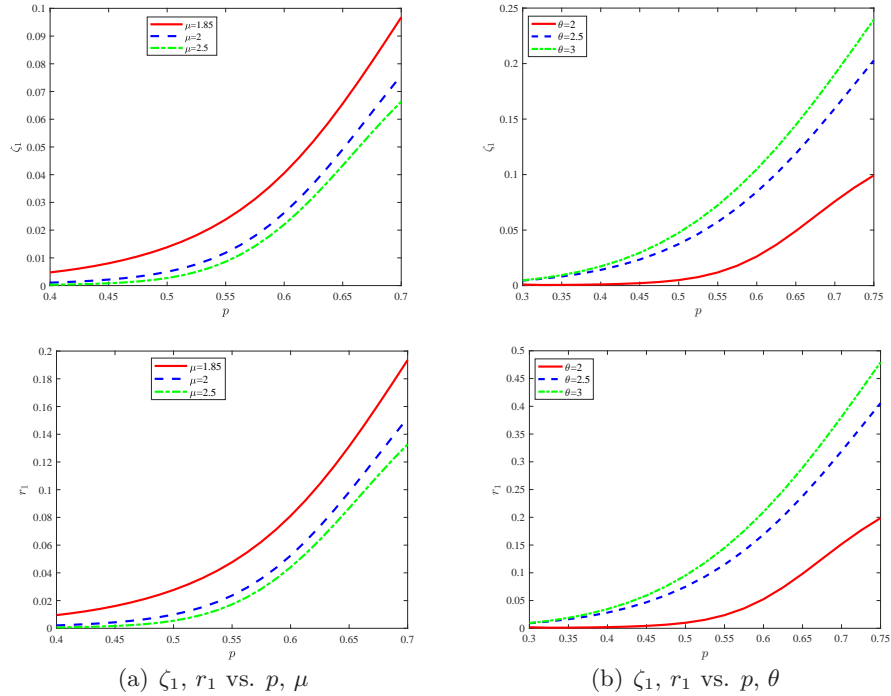


Figure 7: Two performance measures ζ_1 and r_1 vs. three parameters p, μ , and θ .

From Figure 7, it is seen that all ζ_1 and r_1 increase as p increases, which indicates that the stationary probability ζ_1 (or rate r_1) that a transaction package becomes a block can increase as the probability p that a transaction package is approved by each node increases. In addition, we can observe that ζ_1 and r_1 decrease as μ increases in Figure 7(a); while ζ_1 and r_1 increase as θ increases in Figure 7(b). These numerical results indicate that as μ increases, more and more external nodes enter the dynamic PBFT

network, such that the stationary probability ζ_1 (or rate r_1) that a transaction package becomes a block can decrease; while as θ increases, more and more external nodes leave the dynamic PBFT network, such that the stationary probability ζ_1 (or rate r_1) that a transaction package becomes a block can increase. This shows that the number of votable nodes in the dynamic PBFT network significantly affects the stationary probability ζ_1 (or rate r_1) that a transaction package becomes a block. Thus, they are consistent with our intuitive understanding.

In Figure 8, we take the parameters as follows: $\mu = 2$, $\theta = 2$, $\beta = 3$, $p \in [0.375, 0.75]$, and $\gamma = 10, 15, 20$.

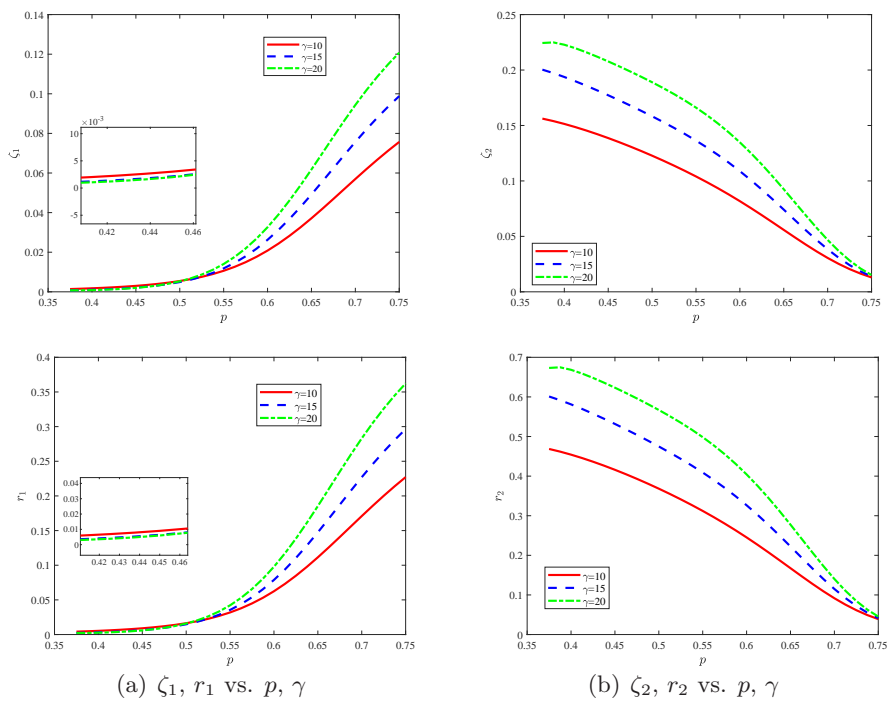


Figure 8: Four performance measures ζ_1 , r_1 , ζ_2 and r_2 vs. two parameters p and γ .

Figure 8(a) shows that ζ_1 and r_1 increase as p increases, sharing the same trends as that in Figure 7; while Figure 8(b) shows that ζ_2 and r_2 decrease as p increases. These numerical results indicate that the stationary probability ζ_1 (or rate r_1) that a transaction package becomes a block increases as the probability p that a package is approved by each node increases; while the stationary probability ζ_2 (or rate r_2) that a transaction package becomes an orphan block decreases as the probability p that a package is approved by each node increases. At the same time, from Figure 8(a), we can see that there exists

a p_0 such that ζ_1 and r_1 decrease as γ increases when $p < p_0$. This shows that the faster the votable nodes vote, the lower the stationary probability ζ_1 (or rate r_1) that the transaction package is approved as a block. On the other hand, ζ_1 and r_1 increase as γ increases when $p > p_0$. This shows that the faster the votable nodes vote, the greater the stationary probability ζ_1 (or rate r_1) that the transaction package is approved as a block. In addition, as can be seen from Figure 8(b), ζ_2 and r_2 increase as γ increases. This shows that the faster the votable nodes vote, the greater the stationary probability ζ_1 (or rate r_1) that the transaction package is refused as an orphan block. These numerical results are also in line with our intuitive understanding.

In Figure 9, we take the parameters as follows: $\mu = 2$, $\theta = 2$, $\gamma = 10$, $p \in [0.35, 0.7]$, and $\beta = 2.5, 3, 3.5$.

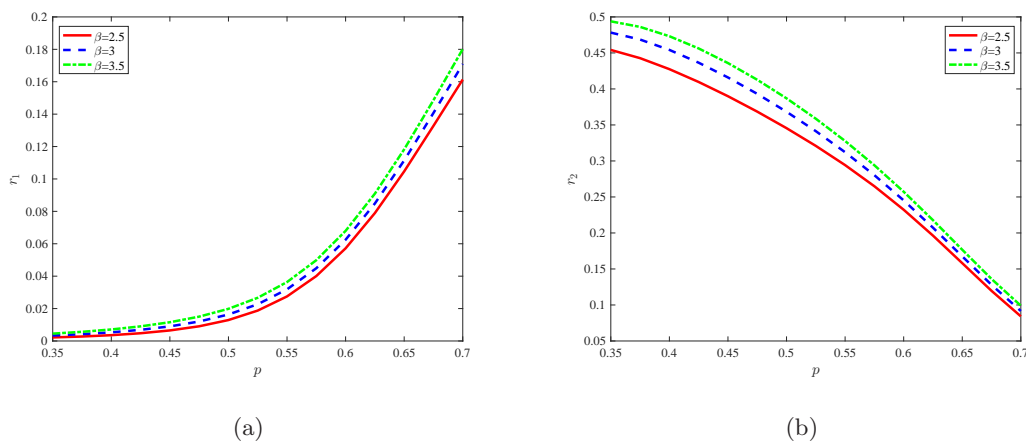


Figure 9: Two performance measures r_1 and r_2 vs. two parameters p and β .

As shown in Figure 9(a), r_1 increases as p increases; while Figure 9(b) suggests r_2 decreases as p increases. At the same time, we can see that r_1 and r_2 increase as β increases, which indicates that the lower the rate β that the network latency of the dynamic PBFT blockchain system, the faster the rate r_1 or r_2 that the transaction packages are pegged on the blockchain or are returned to the transaction pool. Such a numerical result is consistent with our intuitive understanding.

Group two: The dynamic PBFT blockchain system

We observe the impact of $\lambda, b, \mu, \theta, \gamma, p, \beta$ on the performance measures of the dynamic PBFT blockchain system.

Firstly, we explore the impact of λ and b on the η_1 , η_2 and TH. To this end, we take

the some parameters as follows: $r_1 = 0.7$, $r_2 = 0.1$, $b \in [50, 250]$, and $\lambda = 1, 5, 9$.

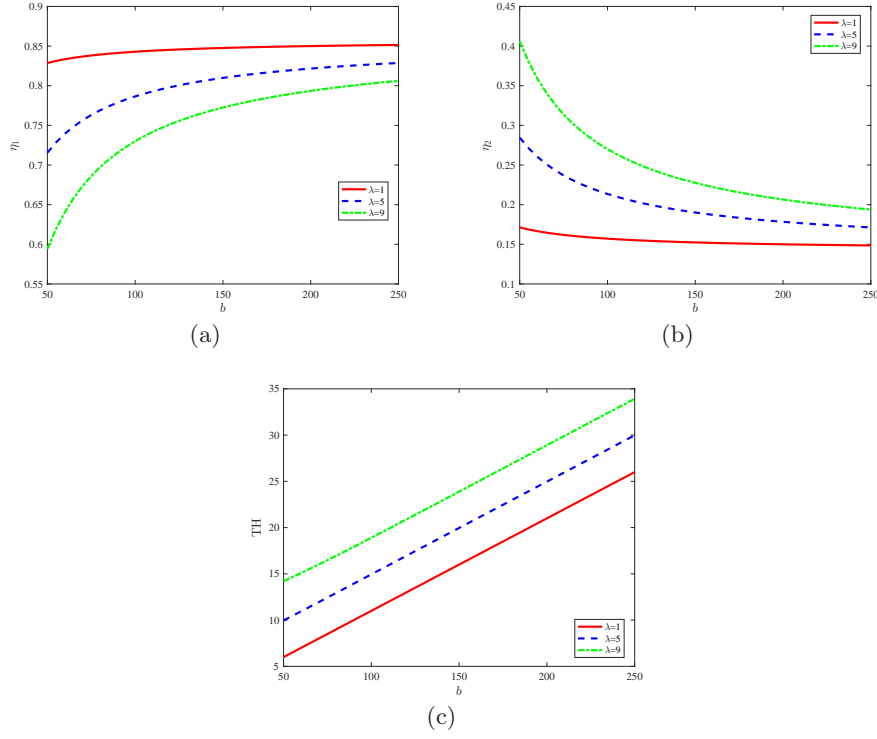


Figure 10: Three performance measures η_1 , η_2 and TH vs. two parameters b and λ .

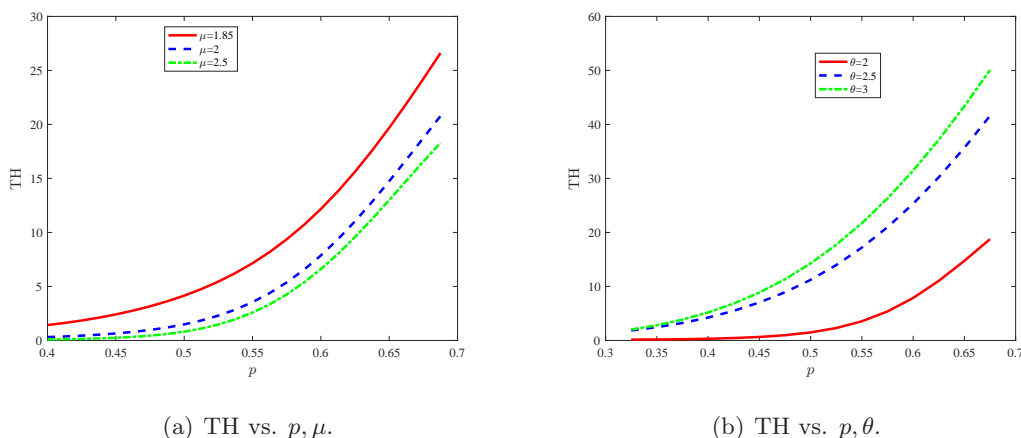
From Figure 10, we can see that η_1 in Figure 10(a) and TH in Figure 10(c) increase as b increases; while η_2 in Figure 10(c) decreases as b increases. Such numerical results indicate that the larger the batch size b is, the greater the probability η_1 of no transaction package, the smaller the probability η_2 of the existing transaction package, and the greater the throughput TH of the dynamic PBFT blockchain system. In other words, as b increases, the probability that the dynamic PBFT blockchain system is in the idle period increases; while the probability that the dynamic PBFT blockchain system is in the busy period decreases; however, the throughput of the dynamic PBFT blockchain system does not decrease accordingly.

Meanwhile, η_1 decreases as λ increases, while η_2 and TH increase as λ increases. This indicates that as λ increases, more and more transactions arrive in the dynamic PBFT blockchain system, this decreases the probability η_1 of no transaction package, increases the probability η_2 of existing transaction package, and improves the throughput TH of the dynamic PBFT blockchain system. Such numerical results are also consistent with our

intuitive understanding.

Secondly, we show the impact of $\mu, \theta, \gamma, p, \beta$ on TH. To this end, we take $\lambda = 10$, $b = 150$ for all the following numerical examples.

In Figure 11(a), we take the parameters: $\theta = 2$, $\beta = 2$, $\gamma = 10$, $p \in [0.4, 0.6875]$, and $\mu = 1.85, 2, 2.5$. In Figure 11(b), we take the parameters: $\mu = 2$, $\beta = 2$, $\gamma = 10$, $p \in [0.325, 0.675]$, and $\theta = 2.5, 3, 3.5$.



(a) TH vs. p, μ .

(b) TH vs. p, θ .

Figure 11: TH vs. p, μ, θ .

From Figure 11(a), we can see that TH decreases as μ increases; while from Figure 11(b), we can see that TH increases as θ increases. These findings indicate that the faster the nodes enter the dynamic PBFT network, the lower the transaction throughput TH of the dynamic PBFT blockchain system; while the faster the nodes leave the dynamic PBFT blockchain system, the greater the transaction throughput TH of the dynamic PBFT blockchain system. In addition, the number of votable nodes affects the throughput of the dynamic PBFT blockchain system. Here, we can get a case: If we aim to pursue the high throughput of the dynamic PBFT blockchain system, we need a small number of votable nodes, but if most of these nodes are Byzantine, the dynamic PBFT blockchain system will be insecure, which means that we sometimes have to sacrifice the throughput to keep the dynamic PBFT blockchain system secure. In addition, from Figure 11, we can see that TH increases as p increases, this is consistent with our intuitive understanding.

In Figure 12, we take the parameters: $\mu = 2$, $\theta = 2$, $\gamma = 10$, $p \in [0.3, 0.6875]$, and $\beta = 2.75, 3, 3.5$. From Figure 12, we can see that TH increases as β increases. This means that the faster the rate of the block-pegging or rolling-back, the greater the transaction

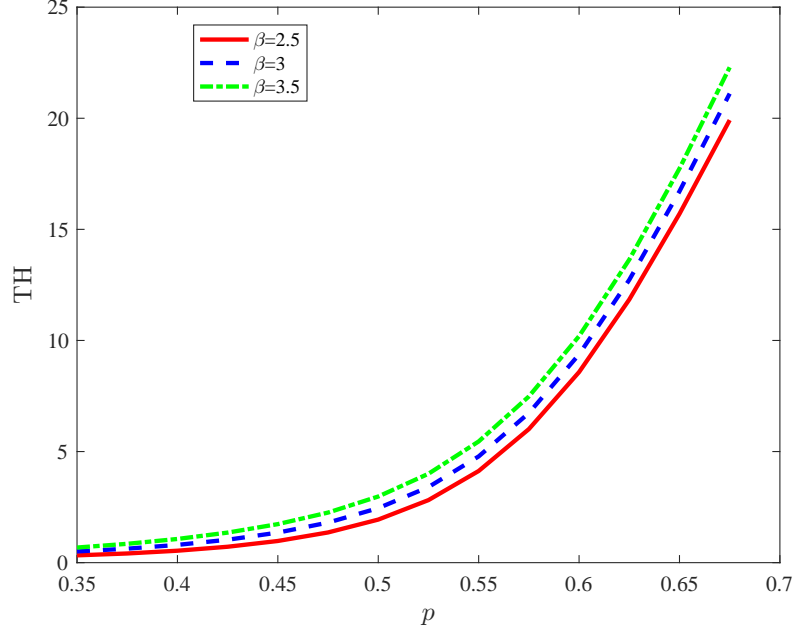


Figure 12: TH vs. p and β .

throughput TH of the dynamic PBFT blockchain system. Such a numerical result is consistent with our intuitive understanding. Meanwhile, from Figure 12, we can see that TH increases as p increases, which has the same trend as that in Figure 11.

In Figure 13, we take the parameters: $\mu = 2$, $\theta = 2$, $\beta = 3$, $p \in [0.325, 0.675]$, and $\gamma = 10, 15, 20$. From Figure 13, we can see that there exists a \tilde{p}_0 such that TH decreases as γ increases when $p < \tilde{p}_0$. This means that the faster the rate of votable nodes voting, the lower the transaction throughput TH of the dynamic PBFT blockchain system. While TH increases as γ increases when $p > \tilde{p}_0$. This means that the faster the rate of node voting, the greater the transaction throughput TH of the dynamic PBFT blockchain system. These numerical results further validate the trends of ζ_1 and r_1 in Figure 8(a). Also, from Figure 13, we can see that TH increases as p increases, which has the same trend as that in Figure 11 as well.

8 Concluding Remarks

In this paper, we first propose a new dynamic PBFT to generalize the ordinary PBFT by introducing new dynamic nodes. That is, the votable nodes may always leave the PBFT

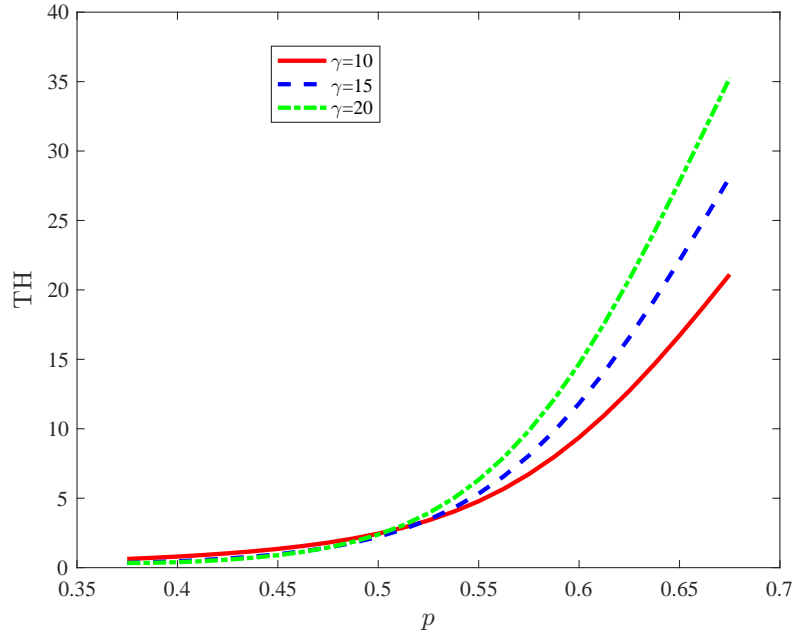


Figure 13: TH vs. p and γ .

network while some new nodes can also enter the PBFT network. Therefore, the number of votable nodes is constantly changing. Then we provide a large-scale Markov modeling technique to analyze the dynamic PBFT voting processes and the dynamic PBFT blockchain system. To this end, we set up a large-scale Markov process and provide key performance analysis for both the dynamic PBFT voting processes and the dynamic PBFT blockchain system. In particular, we provide two effective algorithms for computing the throughput of the dynamic PBFT blockchain system. Finally, we use numerical examples to check the validity of our theoretical results and indicate how some key system parameters influence the performance measures of the dynamic PBFT voting processes and of the dynamic PBFT blockchain system.

Using the theory of multi-dimensional Markov processes and the RG-factorization technique, we are optimistic that the methodology and results developed in this paper shed light on the study of dynamic PBFT blockchain systems such that a series of promising research can be developed potentially. Along this line, we will continue our future research on several interesting directions as follows:

- Let all the three stages (*prepare*, *commit*, and *reply*) follow different exponential

distributions with rates μ_1 , μ_2 , and μ_3 , respectively. Note that such a generalization is far more difficult than this paper due to some complicated parallel phase-type calculations.

— When the arrivals of new nodes or the departures of votable nodes are a Markovian arrival process (MAP), an interesting future research is to focus on finding effective algorithms for dealing with the multi-dimensional Markov processes with a block structure corresponding to the dynamic PBFT blockchain systems.

— When the arrivals of new nodes or the departures of votable nodes are a renewal process, an interesting future research is to focus on fluid and diffusion approximations of the dynamic PBFT blockchain systems.

— Setting up reward functions with respect to cost structure, transaction fee, block reward, blockchain security and so forth. It is very interesting in our future study to develop stochastic optimization, Markov decision processes and stochastic game models in the study of dynamic PBFT blockchain systems.

Acknowledgment

Quan-Lin Li was supported by the National Natural Science Foundation of China under grants No. 71671158 and 71932002.

References

- [1] Abraham, I., Gueta, G., Malkhi, D., Alvisi, L., Kotla, R., & Martin, J. P. (2017). Revisiting fast practical byzantine fault tolerance. arXiv preprint arXiv:1712.01367.
- [2] Alqahtani, S., & Demirbas, M. (2021). Bottlenecks in blockchain consensus protocols. arXiv preprint arXiv:2103.04234.
- [3] Bains, P. (2022). *Blockchain Consensus Mechanisms: A Primer for Supervisors*. International Monetary Fund.
- [4] Bano, S., Sonnino, A., Al-Bassam, M., Azouvi, S., McCorry, P., Meiklejohn, S., & Danezis, G. (2017). Consensus in the age of blockchains. arXiv preprint arXiv:1711.03936.
- [5] Bashir, I. (2018). *Mastering Blockchain: Distributed Ledger Technology, Decentralization, and Smart Contracts Explained*. Packt Publishing Ltd.

- [6] Belchior, R., Vasconcelos, A., Guerreiro, S., & Correia, M. (2021). A survey on blockchain interoperability: Past, present, and future trends. *ACM Computing Surveys*, 54(8), 1-41.
- [7] Bravo, M., István, Z., & Sit, M. K. (2020). Towards improving the performance of BFT consensus for future permissioned blockchains. arXiv preprint arXiv:2007.12637.
- [8] Bright, L., Taylor, P.G., (1995). Calculating the equilibrium distribution in level dependent quasi-birth-and-death processes. *Stochastic Models* 11(3), 497–525.
- [9] Bright, L., Taylor, P.G., (1997). Equilibrium distributions for level-dependent quasi-birth-and-death processes. *Matrix-Analytic Methods in Stochastic Models*. Marcel Dekker, pp. 359–375.
- [10] Cachin, C., & Vukolić, M. (2017). Blockchain consensus protocols in the wild. arXiv preprint arXiv:1707.01873.
- [11] Carrara, G. R., Burle, L. M., Medeiros, D. S., de Albuquerque, C. V. N., & Mattos, D. M. (2020). Consistency, availability, and partition tolerance in blockchain: a survey on the consensus mechanism over peer-to-peer networking. *Annals of Telecommunications*, 75(3), 163-174.
- [12] Castro, M., & Liskov, B. (1999). Practical Byzantine fault tolerance. In: *Proceedings of the Third Symposium on Operating Systems Design and Implementation*, pp: 173-186.
- [13] Castro, M., & Liskov, B. (2002). Practical Byzantine fault tolerance and proactive recovery. *ACM Transactions on Computer Systems*, 20(4), 398-461.
- [14] Chaudhry, N., & Yousaf, M. M. (2018). Consensus algorithms in blockchain: Comparative analysis, challenges and opportunities. In: *The 12th International Conference on Open Source Systems and Technologies*, pp. 54-63.
- [15] Dai, H. N., Zheng, Z., & Zhang, Y. (2019). Blockchain for Internet of Things: A survey. *IEEE Internet of Things Journal*, 6(5), 8076-8094.
- [16] Ekramifard, A., Amintoosi, H., Seno, A. H., Dehghantanha, A., & Parizi, R. M. (2020). A systematic literature review of integration of blockchain and artificial in-

- telligence. In: *Blockchain Cybersecurity, Trust and Privacy*, pp. 147-160. Springer, Advances in Information Security book series, volume 79.
- [17] Eyal I., Sirer E. G. (2018). Majority is not enough: Bitcoin mining is vulnerable. *Communications of the ACM*, 61(7): 95-102.
- [18] Fan, C., Ghaemi, S., Khazaei, H., & Musilek, P. (2020). Performance evaluation of blockchain systems: A systematic survey. *IEEE Access*, 8, 126927-126950.
- [19] Fauziah, Z., Latifah, H., Omar, X., Khoirunisa, A., & Millah, S. (2020). Application of blockchain technology in smart contracts: A systematic literature review. *Aptisi Transactions on Technopreneurship*, 2(2), 160-166.
- [20] Ferdous, M. S., Chowdhury, M. J. M., Hoque, M. A., & Colman, A. (2020). Blockchain consensus algorithms: A survey. arXiv preprint arXiv:2001.07091.
- [21] Fu, X., Wang, H., & Shi, P. (2021). A survey of Blockchain consensus algorithms: mechanism, design and applications. *Science China Information Sciences*, 64(2), 1-15.
- [22] Garcia, R. D., Ramachandran, G., & Ueyama, J. (2022). Exploiting smart contracts in PBFT-based blockchains: A case study in medical prescription system. *Computer Networks*, 211, 109003.
- [23] Göbel, J., Keeler, H. P., Krzesinski, A. E., & Taylor, P. G. (2016). Bitcoin blockchain dynamics: The selfish-mine strategy in the presence of propagation delay. *Performance Evaluation*, 104, 23-41.
- [24] Gorbunova, M., Masek, P., Komarov, M., & Ometov, A. (2022). Distributed ledger technology: State-of-the-art and current challenges. *Computer Science and Information Systems*, 19(1), 65-85.
- [25] Gorkhali, A., Li, L., Shrestha A. (2020). Blockchain: A literature review. *Journal of Management Analytics*, 7(3): 321-343.
- [26] Gueta, G. G., Abraham, I., Grossman, S., et al. (2019). Sbft: a scalable and decentralized trust infrastructure. In: *The 49th Annual IEEE/IFIP International Conference on Dependable Systems and Networks*, pp. 568-580.

- [27] Hao, X., Yu, L., Liu, Z., Zhen, L., & Dawu, G. (2018). Dynamic practical byzantine fault tolerance. In: *The 2018 IEEE Conference on Communications and Network Security*, pp. 1-8.
- [28] Huang, H., Kong, W., Zhou, S., Zheng, Z., & Guo, S. (2021). A survey of state-of-the-art on blockchains: Theories, modelings, and tools. *ACM Computing Surveys*, 54(2), 1-42.
- [29] Javier, K., & Fralix, B. (2020). A further study of some Markovian Bitcoin models from Göbel et al.. *Stochastic Models*, 36(2), 223-250.
- [30] Khamar, J., & Patel, H. (2021). An extensive survey on consensus mechanisms for blockchain technology. In: *Data Science and Intelligent Applications*, pp. 363-374. Springer, Lecture Notes on Data Engineering and Communications Technologies book series, volume 52.
- [31] Kiayias, A., & Russell, A. (2018). Ouroboros-BFT: A simple Byzantine fault tolerant consensus protocol. IACR Cryptol. ePrint Arch. 1049. <https://eprint.iacr.org/2018/1049.pdf>.
- [32] Lamport, L. (1983). The weak Byzantine generals problem. *Journal of the ACM*, 30(3), 668-676.
- [33] Lamport, L. Shostak, R., & Pease, M. (1982) The Byzantine generals problem. *ACM Transactions on Programming Languages and Systems*, 4(3), 382-401.
- [34] Lashkari, B., & Musilek, P. (2021). A comprehensive review of blockchain consensus mechanisms. *IEEE Access*, 9, 43620-43652.
- [35] Leonardos, S., Reijsbergen, D., & Piliouras, G. (2020). Presto: A systematic framework for blockchain consensus protocols. *IEEE Transactions on Engineering Management*, 67(4), 1028-1044.
- [36] Li, Q. L. (2010). *Constructive Computation in Stochastic Models with Applications: The RG-Factorizations*. Springer.
- [37] Li, Q. L., Chang, Y. X., Wu, X., & Zhang, G. (2020). A new theoretical framework of pyramid markov processes for blockchain selfish mining. arXiv preprint arXiv:2007.01459.

- [38] Li, Q. L., Ma, J. Y., & Chang, Y. X. (2018). Blockchain queue theory. In: *International Conference on Computational Social Networks*, pp. 25-40. Springer, Lecture Notes in Computer Science book series, volume 11280.
- [39] Li, Q. L., Ma, J. Y., Chang, Y. X., Ma, F. Q., & Yu, H. B. (2019). Markov processes in blockchain systems. *Computational Social Networks*, 6(1), 1-28.
- [40] Li, Y., Qiao, L., & Lv, Z. (2021). An optimized byzantine fault tolerance algorithm for consortium blockchain. *Peer-to-Peer Networking and Applications*, 14(5), 2826-2839.
- [41] Ma, F. Q., Li, Q. L., Liu, Y. H., & Chang, Y. X. (2022). Stochastic performance modeling for practical byzantine fault tolerance consensus in the blockchain. *Peer-to-Peer Networking and Applications*, online publication, pp. 1-13.
- [42] Maleh, Y., Shojafar, M., Alazab, M., & Romdhani, I. (Eds.). (2020). *Blockchain for Cybersecurity and Privacy: Architectures, Challenges, and Applications*. CRC Press.
- [43] Malkhi, D., Nayak, K., & Ren, L. (2019). Flexible byzantine fault tolerance. In: *Proceedings of the 2019 ACM SIGSAC Conference on Computer and Communications Security*, pp. 1041-1053.
- [44] Martin, J. P., & Alvisi, L. (2006). Fast Byzantine consensus. *IEEE Transactions on Dependable and Secure Computing*, 3(3), 202-215.
- [45] Meshcheryakov, Y., Melman, A., Evsutin, O., Morozov, V., & Koucheryavy, Y. (2021). On performance of PBFT for IoT-applications with constrained devices. arXiv preprint arXiv:2104.05026.
- [46] Nakamoto, S. (2008). Bitcoin: A peer-to-peer electronic cash system. 1-9. <http://bitcoin.org/bitcoin.pdf> .
- [47] Navaroj, G. I., Julie, E. G., & Robinson, Y. H. (2022). Adaptive practical Byzantine fault tolerance consensus algorithm in permission blockchain network. *International Journal of Web and Grid Services*, 18(1), 62-82.
- [48] Narayanan, A., Bonneau, J., Felten, E., Miller, A., & Goldfeder, S. (2016). *Bitcoin and Cryptocurrency Technologies: A Comprehensive Introduction*. Princeton University Press.

- [49] Natoli, C., Yu, J., Gramoli, V., & Esteves-Verissimo, P. (2019). Deconstructing blockchains: A comprehensive survey on consensus, membership and structure. arXiv preprint arXiv:1908.08316.
- [50] Neuts, M. F. (1981). *Matrix-Geometric Solutions in Stochastic Models: An Algorithmic Approach*. The Johns Hopkins University Press.
- [51] Nguyen, G. T., & Kim, K. (2018). A survey about consensus algorithms used in blockchain. *Journal of Information processing systems*, 14(1), 101-128.
- [52] Nguyen, C. T., Hoang, D. T., Nguyen, D. N., Niyato, D., Nguyen, H. T., & Dutkiewicz, E. (2019). Proof-of-stake consensus mechanisms for future blockchain networks: fundamentals, applications and opportunities. *IEEE Access*, 7, 85727-85745.
- [53] Nijse, J., & Litchfield, A. (2020). A taxonomy of blockchain consensus methods. *Cryptography*, 4(4), 32.
- [54] Nischwitz, M., Esche, M., & Tschorsch, F. (2021). Bernoulli meets PBFT: Modeling BFT protocols in the presence of dynamic failures. In: *2021 16th Conference on Computer Science and Intelligence Systems* (pp. 291-300). IEEE.
- [55] Oliveira, A., Moniz, H., & Rodrigues, R. (2022). Alea-BFT: Practical asynchronous Byzantine fault tolerance. arXiv preprint arXiv:2202.02071.
- [56] Ongaro, D., & Ousterhout, J. (2014). In search of an understandable consensus algorithm. In: *Proceedings of 2014 USENIX Annual Technical Conference*, pp. 305-319.
- [57] Oyinloye, D. P., Teh, J. S., Jamil, N., & Alawida, M. (2021). Blockchain consensus: An overview of alternative protocols. *Symmetry*, 13(8), 1363.
- [58] Pahlajani, S., Kshirsagar, A., & Pachghare, V. (2019). Survey on private blockchain consensus algorithms. In: *The 1st International Conference on Innovations in Information and Communication Technology*, pp. 1-6.
- [59] Pease, M., Shostak, R., & Lamport, L. (1980). Reaching agreement in the presence of faults. *Journal of the ACM*, 27(2), 228-234.
- [60] Raj, K. (2019). *Foundations of Blockchain: The Pathway to Cryptocurrencies and Decentralized Blockchain Applications*. Packt Publishing Ltd.

- [61] Rehan, M. M., & Rehmani, M. H. (Eds.). (2020). *Blockchain-Enabled Fog and Edge Computing: Concepts, Architectures and Applications*. CRC Press.
- [62] Reischuk, R. (1985). A new solution for the Byzantine generals problem. *Information and Control*, 64(1-3), 23-42.
- [63] Sakho, S., Zhang, J., Essaf, F., Badiss, K., Abide, T., & Kiprop, J. K. (2020). Research on an improved practical byzantine fault tolerance algorithm. In: *The 2nd International Conference on Advances in Computer Technology, Information Science and Communications*, pp. 176-181.
- [64] Salimitari, M., & Chatterjee, M. (2018). A survey on consensus protocols in blockchain for iot networks. arXiv preprint arXiv:1809.05613.
- [65] Schar, F., & Berentsen, A. (2020). *Bitcoin, Blockchain, and Cryptoassets: A Comprehensive Introduction*. MIT Press.
- [66] Schlichting, R. D., & Schneider, F. B. (1983). Fail-stop processors: An approach to designing fault-tolerant computing systems. *ACM Transactions on Computer Systems*, 1(3), 222-238.
- [67] Sharma, P., Jindal, R., & Borah, M. D. (2020). Blockchain technology for cloud storage: A systematic literature review. *ACM Computing Surveys*, 53(4), 1-32.
- [68] Smetanin, S., Ometov, A., Komarov, M., Masek, P., & Koucheryavy, Y. (2020). Blockchain evaluation approaches: State-of-the-art and future perspective. *Sensors*, 20(12), 3358.
- [69] Song, X. S., Li, Q. L., Chang, Y. X., & Zhan, C. (2022). A Markov process theory for network growth processes of DAG-based blockchain systems. arXiv preprint arXiv:2209.01458.
- [70] Stifter, N., Judmayer, A., & Weippl, E. (2019). Revisiting practical byzantine fault tolerance through blockchain technologies. In: *Security and Quality in Cyber-Physical Systems Engineering*, pp. 471-495. Springer.
- [71] Thai, Q. T., Yim, J. C., Yoo, T. W., Yoo, H. K., Kwak, J. Y., & Kim, S. M. (2019). Hierarchical Byzantine fault-tolerance protocol for permissioned blockchain systems. *The Journal of Supercomputing*, 75(11), 7337-7365.

- [72] Veronese, G. S., Correia, M., Bessani, A. N., Lung, L. C., & Verissimo, P. (2011). Efficient Byzantine fault-tolerance. *IEEE Transactions on Computers*, 62(1), 16-30.
- [73] Wan, S., Li, M., Liu, G., & Wang, C. (2020). Recent advances in consensus protocols for blockchain: a survey. *Wireless networks*, 26(8), 5579-5593.
- [74] Wang, W., Hoang, D. T., Hu, P. et al. (2019). A survey on consensus mechanisms and mining strategy management in blockchain networks. *IEEE Access*, 7, 22328-22370.
- [75] Xiao, Y., Zhang, N., Lou, W., & Hou, Y. T. (2020). A survey of distributed consensus protocols for blockchain networks. *IEEE Communications Surveys & Tutorials*, 22(2), 1432-1465.
- [76] Xiong, H., Chen, M., Wu, C., Zhao, Y., & Yi, W. (2022). Research on Progress of Blockchain Consensus Algorithm: A Review on Recent Progress of Blockchain Consensus Algorithms. *Future Internet*, 14(2), 47.
- [77] Yao, W., Ye, J., Murimi, R., & Wang, G. (2021). A survey on consortium blockchain consensus mechanisms. arXiv preprint arXiv:2102.12058.
- [78] Zhan, Y., Wang, B., Lu, R., & Yu, Y. (2021). DRBFT: Delegated randomization Byzantine fault tolerance consensus protocol for blockchains. *Information Sciences*, 559, 8-21.